Redox Biology 19 (2018) 388–400

Contents lists available at ScienceDirect

Redox Biology

journal homepage: www.elsevier.com/locate/redox

Research Paper

Chlorination and oxidation of human plasma fibronectin by myeloperoxidase-derived oxidants, and its consequences for smooth muscle cell function

Tina Nybo[a], Huan Cai[a], Christine Y. Chuang[a], Luke F. Gamon[a], Adelina Rogowska-Wrzesinska[b], Michael J. Davies[a,*]

[a] Department of Biomedical Sciences, Panum Institute, University of Copenhagen, Copenhagen, Denmark
[b] Department of Biochemistry and Molecular Biology and VILLUM Center for Bioanalytical Sciences, University of Southern Denmark, Odense, Denmark

ARTICLE INFO

Keywords:
Fibronectin
Myeloperoxidase
Hypochlorous acid
3-chlorotyrosine
Oxidation
Chlorination
Extracellular matrix
Vascular smooth muscle cells

ABSTRACT

Fibronectin (FN) occurs as both a soluble form, in plasma and at sites of tissue injury, and a cellular form in tissue extracellular matrices (ECM). FN is critical to wound repair, ECM structure and assembly, cell adhesion and proliferation. FN is reported to play a critical role in the development, progression and stability of cardiovascular atherosclerotic lesions, with high FN levels associated with a thick fibrotic cap, stable disease and a low risk of rupture. Evidence has been presented for FN modification by inflammatory oxidants, and particularly myeloperoxidase (MPO)-derived species including hypochlorous acid (HOCl). The targets and consequences of FN modification are poorly understood. Here we show, using a newly-developed MS protocol, that HOCl and an enzymatic MPO system, generate site-specific dose-dependent Tyr chlorination and dichlorination (up to 16 of 100 residues modified), and oxidation of Trp (7 of 39 residues), Met (3 of 26) and His (1 of 55) within selected FN domains, and particularly the heparin- and cell-binding regions. These alterations increase FN binding to heparin-containing columns. Studies using primary human coronary artery smooth muscle cells (HCASMC) show that exposure to HOCl-modified FN, results in decreased adherence, increased proliferation and altered expression of genes involved in ECM synthesis and remodelling. These findings indicate that the presence of modified fibronectin may play a major role in the formation, development and stabilisation of fibrous caps in atherosclerotic lesions and may play a key role in the switching of quiescent contractile smooth muscle cells to a migratory, synthetic and proliferative phenotype.

1. Introduction

Fibronectin (FN) is a large plasma and extracellular matrix glycoprotein, composed of two nearly identical subunits (~ 230–270 kDa) linked by two disulfide-bonds located near the carboxyl termini [1,2]. The protein exists in two forms: a soluble form predominantly found in plasma, but also in abundance at sites of tissue injury, and a cellular form present in tissue extracellular matrix (ECM). The plasma form plays a key role in the early physiological responses to tissue injury as it binds to fibrin fibres via multiple domains and hence is a key component of blood clots [3]. The resulting fibrin-FN network supports migration and adhesion of fibroblast and endothelial cells which over time replace this provisional matrix structure with cell-derived FN, collagen, laminins and other ECM components [4,5]. Cell-derived FN, which is synthesized by endothelial, smooth muscle and fibroblast cells, amongst others, is structurally-related to the plasma form, but also contains extra domains (extra domains A and B) which are alternatively spliced type III modules that are not present in the plasma form [6].

FN is present in the ECM of the arterial wall under normal physiological conditions [7], but a significant increase in concentration, and different isoforms, have been reported in atherosclerotic lesions [8]; these changes appear to occur during lesion development [9]. Patients with coronary artery disease also have elevated levels of plasma FN [10]. These changes may be associated with remodelling of the vascular

Abbreviations: 3-ClTyr, 3-chlorotyrosine; 3,5-Cl_2Tyr, 3,5-dichlorotyrosine; ECM, extracellular matrix; ELISA, enzyme-linked immunosorbent assay; FN, human plasma fibronectin; HCASMC, human coronary artery smooth muscle cells; HOCl, the physiological mixture of hypochlorous acid and its anion $^{-}$OCl; MCD, monochlorodimedone; MPO, myeloperoxidase; MSA, methanesulfonic acid; RSO, relative site occupancy; SDC, sodium deoxycholate; SMC, smooth muscle cell; TCA, trichloroacetic acid; TFA, trifluoroacetic acid; TMB, 3,3′,5,5′-tetramethylbenzidine

* Corresponding author.
E-mail address: davies@sund.ku.dk (M.J. Davies).

https://doi.org/10.1016/j.redox.2018.09.005
Received 31 July 2018; Received in revised form 28 August 2018; Accepted 3 September 2018
Available online 05 September 2018

wall during the development of atherosclerosis, with considerable evidence for increased ECM deposition in the fibrous caps of atherosclerotic plaques [11]. The formation of a thick fibrous cap is widely regarded as being beneficial with regard to plaque stability [11]. Rupture of the lesion, exposure of the highly thrombogenic substrata, and subsequent thrombus formation, is a major cause of heart attacks and strokes [11]. Rupture prone plaques typically have a thin fibrous cap, increased numbers of activated inflammatory cells capable of producing oxidants, high levels of lipids, and low numbers of smooth muscle cells [12,13]. Rupture occurs most commonly in the shoulder regions where macrophages and other leukocytes accumulate [14,15]. Studies on atherosclerosis-prone apo $E^{-/-}$ mice that do not express plasma-derived FN, have shown a reduction in number and size of atherosclerotic lesions, however mice deficient in plasma-derived FN lacked vascular smooth muscle cell infiltration and failed to develop a fibrous cap [16]. These data are consistent with the hypothesis that FN plays a critical role in generating and stabilizing the fibrous cap of atherosclerotic lesions, and plays a major role in determining lesion stability and propensity to rupture. The colocalization of inflammatory cells with FN in plaque shoulder regions, and FN degradation during the progression of atherosclerosis, supports the hypothesis that plaques are damaged and destabilized by inflammatory cell oxidants, with this occurring, at least in part, via ECM damage [17,18].

Oxidants are intentionally generated during many physiologic and pathological processes [19]. Activated leukocytes generate superoxide radicals ($O_2^{\bullet-}$) and hydrogen peroxide (H_2O_2) via NADPH oxidase (NOX) enzymes, and neutrophils, monocytes and some tissue macrophages release the heme enzyme myeloperoxidase (MPO) from intracellular storage granules [20]. In the presence of chloride ions (Cl^-), MPO utilizes H_2O_2 to generate the potent oxidant hypochlorous acid (HOCl) [20,21]. HOCl reacts rapidly with many biological targets, with kinetic data indicating that proteins are major targets, due to their abundance and high reactivity [21,22]. Although HOCl plays an important role in killing invading pathogens, excessive or misplaced generation can result in host tissue damage, with this being associated with multiple human pathologies involving acute or chronic inflammation, including atherosclerosis [21,23–25].

There is limited data on HOCl-induced modifications to isolated FN, or FN in the arterial wall, though it is known that FN can be modified by HOCl both *in vitro,* and in basement membrane preparations from other tissues [26–28]. Modified FN colocalizes with leukocyte-derived MPO in human atherosclerotic lesions [29], but the nature of the modifications induced on FN by MPO-derived oxidants are unknown. Sulfur-containing amino acids (Cys, Met and cystine) are major targets for HOCl [22,30,31], however FN has low levels of Cys, though a large number of Met and disulfide (cystine) bonds; these are therefore likely to be major targets, if they are accessible. HOCl can also modify His, Trp, Lys and Tyr residues [22] though the chloramines (RNHCl species) formed on His and Lys have limited stability and hence cannot be easily quantified *in vivo* [32,33]. Reaction of HOCl and chloramines with Tyr generates the well-established biomarker 3-chlorotyrosine (3Cl-Tyr) [34–36]. This stable product is characteristic of MPO-mediated damage, as it is the only enzyme known to induce significant levels of chlorination [35]. Elevated 3Cl-Tyr levels have been detected on low- and high-density lipoproteins extracted from atherosclerotic lesions, and also on plasma proteins from people with cardiovascular disease [36–40].

The studies reported here aimed to determine whether human plasma FN is susceptible to damage induced by HOCl and a MPO-catalysed system, to identify the nature and sites of damage using a recently developed proteomics approach [41], and to examine whether oxidant-modified FN has functional effects on human coronary artery smooth muscle cells, a key cell type within the artery wall.

2. Materials and methods

2.1. Materials

All chemicals were purchased from Sigma Aldrich except for: human plasma fibronectin (FN) (Corning or Sigma-Aldrich), human myeloperoxidase (Planta Natural Products), lysyl endopeptidase (Lys-C) (Wako), and 3-chloro-[$^{13}C_6$] tyrosine (Cambridge Isotope Laboratories). All solvents were HPLC or LCMS grade. RNA was extracted from cell cultures using an RNeasy kit (Qiagen, Valencia, CA) according to the manufacturers protocol, with cDNA synthesis and quantitative real-time PCR carried out using SuperScript™ III First-Strand Synthesis SuperMix (Invitrogen) and SYBR® GreenER™ qPCR SuperMix Universal (Invitrogen), respectively. Human interleukin-6 (IL-6) was determined using an ELISA kit (Biolegend; San Diego, USA) as described by the manufacturer. Human coronary artery smooth muscle cells (donor 1596), SMC growth medium and SMC basal medium were from Cell Applications (San Diego, USA).

2.2. Quantification of HOCl formation using 3,3′,5,5′-tetramethylbenzidine (TMB) or monochlorodimedone (MCD)

TMB was used to quantify HOCl production by the MPO-H_2O_2-Cl^- system as outlined previously [42]. The developing reagent consisted of 20 mM TMB in dimethylformamide, and 2 mM NaI in sodium acetate buffer (0.44 M, pH 5.4) prepared immediately prior to use. The MPO-H_2O_2-Cl^- (20 nM MPO, 0–200 μM H_2O_2, 200 mM Cl^-) or reagent HOCl (0–200 μM) was incubated with taurine (10 mM) at 37 °C for 2 h. Then, 50 μL of TMB reagent was added to each well and incubated for 5 min at 21 °C. The absorbance at 645 nm was then measured on a Spectra Max® i3x microplate reader. The concentration of HOCl formed and trapped by taurine, was calculated using a standard curve generated using reagent HOCl (0–200 μM). HOCl production was also quantified by determining the loss of parent MCD spectrophotometrically, using a molar extinction coefficient ε_{290} 17,700 M^{-1} cm^{-1} [43].

2.3. Oxidation of human plasma fibronectin (FN)

Purified FN was prepared in 100 mM sodium phosphate buffer, pH 7.4, at a concentration of 1 mg mL^{-1} (2.27 μM). HOCl was added at 0, 100 or 500 μM and incubated for 1 h at 21 °C. HOCl stocks were quantified spectrophotometrically at 292 nm using a molar extinction coefficient (ε_{292}) of 350 M^{-1} cm^{-1}. For MPO-mediated oxidation, aliquots of FN were incubated (unless otherwise indicated) with 0.1 μM MPO, 100 mM NaCl and 500 μM H_2O_2, with the H_2O_2 added as 10 × 50 μM aliquots at 10 min intervals at 37 °C on a thermo-shaker, and incubated for a further 10 min after the final addition. Controls with no MPO, no H_2O_2, no NaCl, and untreated FN were included.

2.4. Protein digestion for mass spectrometry

Modified and non-modified proteins were digested in-solution using an optimised protocol without the use of reduction and alkylation, as these reduce the yield of chlorinated products (T. Nybo, M.J. Davies, A. Rogowska-Wrzesinska, unpublished data). Briefly, residual reactants and salts were removed using 10 kDa spin-filters (Amicon Ultra-0.5 Ultracel-10K, Merck Millipore, Ireland), with buffer exchange into 50 mM triethyl ammonium bicarbonate buffer supplemented with 4 M urea and 1% sodium deoxycholate (SDC) to induce denaturation. Proteins were incubated for > 3 h, followed by a two-step digestion using Lys-C for 2 h in 4 M urea, followed by trypsin for 18 h in 1 M urea. The temperature was kept at 30 °C to minimize protein carbamylation. SDC was removed using acidification and ethyl acetate phase transfer as described previously [44].

2.5. Mass spectrometry analysis of treated samples

One μg of peptide mixture was separated using a precolumn (5 μm particle size, C18 fused silica beads, 4 cm × 100 μm ID) coupled to an analytical column (3 μm particle size, C18 fused silica beads, 20 cm × 75 μm ID) mounted on an EASY nLC 1000 instrument (Thermo Fisher Scientific, Germany). Peptides were separated at a flow rate of 250 nL min^{-1} using buffer A (0.1% formic acid) with 5–38% buffer B (0.1% formic acid, 90% acetonitrile), over a 60 min linear gradient, followed by an 8 min wash, using increasing concentrations of buffer B (38–100%), and 5 min of 100% buffer B. Eluting peptides were analysed on a QExactive HF (Thermo Fisher Scientific) mass spectrometer in positive ion mode using data-dependent acquisition. Full scans of m/z 400–1400 was recorded with 120,000 resolution, with the top 12 most intense ions selected for higher energy collisional dissociation (HCD) fragmentation at a normalised collision energy of 28. Blanks were run between each sample to monitor and prevent carry-over.

2.6. Relative quantification of oxidative modifications by mass spectrometry

Mass spectrometry results (.raw, Xcalibur data files) were imported and analysed using Progenesis QI for proteomics (Nonlinear Dynamics, USA). Database searches were carried out using Proteome Discoverer 2.1 against a FN isoform database. For MPO-mediated oxidations, MPO isoform sequences were included in the database. The following search parameters were used: parent ion tolerance - 4 ppm; fragment ion tolerance - 0.1 Da; trypsin - 2 missed cleavages allowed; fixed modifications – none; variable modifications: Cl (Y, W), 2 x Cl (Y, W), 1 x O (M, H, C, W), 2 x O (M, C, W), 3 x O (C). The results were exported as pepXML files and imported back into Progenesis. Peptide measurements were exported from Progenesis providing normalised abundance calculated from the extracted ion chromatograms of precursor ions [45]. All identifications were validated by manual inspection of fragment ion spectra and chromatograms. For chlorinated peptides, the isotopic distribution was inspected relative to the native peptide to confirm the characteristic enhancement of the 3rd isotopic isomer arising from the presence of chlorine isotopes [46]. Quantitative values from different charge states were pooled manually. Zero-values from Progenesis were handled in two ways: a) if missing in all replicates, the abundance was assumed to be below the detection limit and for calculation purposes their value was set to 1; b) if missing in 1 replicate but present in the remaining, it was assumed to be randomly missing and removed. The relative site occupancy for modification of a particular amino acid was calculated by dividing the sum of signal intensities (area-under-the-curve) of all peptide spectral matches containing the modified position, with the sum of the intensity of all peptide spectral matches containing the position (non-modified and modified) with the values expressed as a percentage.

2.7. Quantification of total 3-chlorotyrosine levels

Protein samples (25 μg) were precipitated with trichloroacetic acid (TCA; w/v 8%) and spiked with 3-chloro-[$^{13}C_6$]tyrosine (100 pmol, internal standard) before evaporation using a centrifugal vacuum concentrator for 1 h, as described previously [47]. MS experiments using spin filters versus TCA/acetone precipitation for protein purification showed that the use of TCA did not induce artefactual chlorination (T. Nybo, M.J. Davies, A. Rogowska-Wrzesinska, unpublished data). The resulting pellet was hydrolysed overnight in 4 M methanesulfonic acid (MSA, 50 μL) under vacuum at 110 °C. Amino acids were partially purified by solid-phase extraction using 1 mL C-18 cartridges (Supelco). The columns were activated using 100% methanol (1 mL), followed by equilibration with 0.1% trifluoroacetic acid (TFA) in water (2 × 1 mL). Samples were diluted with 1% TFA in water (10 μL hydrolysate in 400 μL of 1% TFA) in order to improve ion-pairing and subsequent binding of amino acids to the C18 material. The samples were loaded onto the column and washed with 0.1% TFA in water (1 × 1 mL) followed by elution with 50% methanol containing 0.1% formic acid (1 × 1 mL). Extracts were dried at 60 °C under vacuum for 4 h and dissolved in 50 μL of 0.1% formic acid.

3-Chlorotyrosine (3-ClTyr) was quantified by electrospray ionisation LC-MS in the positive ion mode using a Bruker Impact HD II mass spectrometer. Samples were separated by gradient elution using a Phenomenex Aeris™ 2.6 μm PEPTIDE XB-C18 250 × 2.1 mm HPLC column. Elution was started at 3% B for 1 min, followed by gradient elution from 3% to 50% B over 9 mins, 50–80% B over 2 min, followed by isocratic elution using 80% B for 3 mins, before decreasing to 3% B over 2 mins and re-equilibration at 3% B for 3 min. Buffer A consisted of 0.1% formic acid in H_2O and buffer B consisted of 90% acetonitrile in H_2O. The electrospray needle was held at 4500 V, with end plate offset of 500 V and temperature of 200 °C. Nitrogen gas was used for both the nebuliser (2.0 bar) and as the dry gas (8.0 L min^{-1}). An external standard curve was generated for 3-ClTyr with a concentration range of 78 fmol to 20 pmol loaded onto the column, with the internal standard maintained at 4 pmol. A linear response of 3-ClTyr relative to the internal standard was observed over this concentration range. Standards were prepared in 0.1% formic acid in H_2O. Spectra were collected in MS1 mode and quantification performed on extracted ion chromatograms for 3-ClTyr (m/z = 216.04) and 3-Cl[$^{13}C_6$]Tyr (m/z = 222.06).

2.8. Heparin-affinity chromatography

FN (100 μg) was loaded onto a HiTrap Heparin High Performance column (GE Healthcare, UK) on a Äkta FPLC system (GE Healthcare, UK) using 10 mM sodium phosphate buffer pH 7.4 at a flow rate of 1 mL min^{-1}. Elution was carried out using a 10 min gradient from 0% to 100% of 100 mM NaCl in 10 mM sodium phosphate buffer, pH 7.4. Protein elution was monitored by UV detection.

2.9. Cell culture

Primary human coronary artery smooth muscle cells (HCASMC) were cultured *in vitro* using commercial smooth muscle cell (SMC) growth medium in a humidified incubator containing 5% CO_2 at 37 °C. HCASMC were cultured for 1 week with an initial density of 10^4 cells in 200 μL of medium in 96-well plate, or at 2 × 10^4 cells in 500 μL of medium in 8-well tissue culture slides, or 10^6 cells in 25 mL medium in T175 flasks. The growth medium was replaced three times per week.

2.10. Adhesion of human coronary artery smooth muscle cells (HCASMC) to native and modified FN

Adhesion of HCASMC to native or modified FN was assessed using black 96-well tissue culture plates pre-coated overnight with purified FN (20 μg mL^{-1}, ~ 44 μM). The plate was then treated with 50 μL of HOCl (1–200 μM) or a MPO-H_2O_2-Cl^- system (20 nM MPO, 1–200 μM H_2O_2, 200 mM Cl^-) for 2 h at 37 °C. The plate was then rinsed twice with sterile PBS to remove any excess oxidant or the enzyme system, before blocking with sterile and heat-denatured 1% BSA in PBS (w/v) at 37 °C for 1 h to minimize non-specific binding of cells to the plastic. The HCASMC (5 × 10^6 cells mL^{-1}) were pre-loaded before use with 5 μM calcein AM for 30 min at 37 °C, with the cells subsequently washed with pre-warmed basal medium to remove residual dye. The calcein AM-labelled HCASMC were then added at a concentration of 10^4 cells per well to the plates containing native or modified FN, and incubated in a tissue culture incubator for 90 min. The plates were then rinsed twice with PBS (containing Ca^{2+} and Mg^{2+}) to remove non-adherent cells. Fluorescence from the adherent cells was then quantified using a SpectraMax® i3x microplate reader, with λ_{ex} 490 nm and λ_{em} 520 nm, respectively. Alternatively, adhesion of HCASMC to modified FN was carried out on 8-well glass slides. These were coated with FN, treated with HOCl (20 or 100 μM), washed, and incubated with HCASMC

(2×10^4 cells per well) as described above. Adherent cells were rinsed twice with PBS and then fixed with 4% formaldehyde in PBS (37 °C, 15 min) then permeabilized using 0.5% (v/v) Triton X-100 in PBS on ice for 5 min. The slides were rinsed again with PBS and counterstained with ActinRed 555 (Life Technologies) and 1 μg mL^{-1} DAPI in PBS in the dark at 21 °C for 30 min to stain F-actin and nuclei, respectively. The cells were then rinsed three times with PBS, air dried, had cover slips added, and examined under a fluorescence microscopy (Olympus, Japan). Alternatively the permeabilized HCASMC (as above) were stained with 0.4% trypan blue for 15 min at 21 °C, to examine cell morphology using bright field microscopy.

2.11. Proliferation of HCASMC on native and modified FN

Black 96-well tissue culture plates coated with native or modified FN were prepared as described above, except the FN was treated with 1 μM HOCl at 37 °C for 2 h. The plates were then rinsed (2 × PBS) to remove residual HOCl, and then blocked with sterile and heat-denatured 1% (w/v) BSA in PBS (Ca^{2+} and Mg^{2+} -free) at 37 °C for 1 h to minimize non-specific binding. HCASMC were pre-loaded with 5 μM calcein AM (as above), and then added (10^4 cells per well) to the native or treated FN and incubated for 90 min. The plates were then rinsed (as above) to remove non-adherent cells. The initial (day 0) density of adherent cells was quantified by fluorescence as described above. The plates were then washed twice with PBS (with Ca^{2+} and Mg^{2+}) and replaced with 200 μL of growth medium, then incubated for 48 h in an incubator. The final cell population (day 2) was determined using the MTS assay: 20 μL of MTS reagent was added to each well and incubated for 4 h. The samples were then transferred to a clear tissue culture plate, and the absorbance at 490 nm measured using a SpectraMax® i3x microplate reader.

2.12. Real-time PCR

Quantitative real time PCR was used to examine mRNA transcription profiles in HCASMC incubated on native FN, or FN treated with HOCl (1, 10, 50 μM). Multiple genes involved in cell mitosis, the inflammation response, and ECM synthesis and turnover were examined. Total RNA was extracted from HCASMC after 48 h incubation on native or HOCl-treated FN using an RNeasy Mini Kit (Qiagen). The RNA concentration and purity was quantified spectrophotometrically using a SpectraMax® i3x microplate reader. RNA (400 ng) was used for single strand cDNA synthesis using a cDNA RT kit in a total volume of 20 μL containing 1 × RT reaction mix, 10 × RT Enzyme Mix, and 2 U RNase H. Conditions for the reverse transcription reactions were as follow: 25 °C for 10 min, 50 °C for 30 min and 85 °C for 5 min. Real-time PCR was carried out on ABI 7900 HT machine with 20 μL reaction mix buffer containing 10 μL SYBR® GreenER™, 2 μL of each primer at 10 pmol/μL, 0.4 μL of ROX reference dye and 2 μL of cDNA. Commercial primers were ordered form Qiagen without definite primer sequence (*IL-6*, *TNF-α*, *COX-2, iNOS, IL-1β, FN1, COL4A1, LAMA1, LAMA5, LAMB2*), other primers were also used (5′-3′): *PCNA* (F: AGGCACTCAAGGACCTCA TCA; R: GAGTCCATGCTCTGCAGGTTT), *CCNA1* (F: GCACCCTGCTCG TCACTTG; R: CAGCCCCCAATAAAAGATCCA), *CCNB1* (F: AGCTGCTG CCTGGTGAAGAG; R: GCCATGTTGATCTTCGCCTTA), *LAMA2* (F: GTT CCAGGGCATTTGTGTGA; R: TAGATGCTGGGTTTGGGCTTT), *MMP1* (F: CGCACAAATCCCTTCTACCC; R: GGACTTCATCTCTGTCGGC), *MMP11* (F: TCTACTGGAAGTTTGACCCTGTG; R: GTCAGAGGAAAGTGTTGG CAG), *MMP13* (F: TTTTTCAACGGACCCATACAGTT; R: TTACCCCAAA TGCTCTTCAGG), *ADAMTS1* (F: CTTGTGGCAGACCAGTCGAT; R: TTC ACCACCACCAGGCTAAC), *TIMP2* (F: TACACACGCCAATGAAACCGA; R: GGTTGCCGCTGAATAGAACA). *β-actin* (F: GATTCCTATGTGGGCGA CGA; R: AGTTGGTGACGATGCCGTG) was used as house-keeping gene. Triplicate wells were used and data analysis was carried out using the $2^{-\Delta\Delta CT}$ method.

2.13. Statistics

Statistical analysis of MS data was performed by Student's *t*-test using SAS Enterprise Guide 7.1 (SAS Inc., USA). For other analyses, one-way ANOVA and Student's *t*-tests were performed on IBM SPSS 19.0 to examine statistical significance. Experiments were performed in triplicate and $P < 0.05$ was considered significant.

3. Results

3.1. Hypochlorous acid induces chlorination and oxidation of human plasma FN

To investigate the effect of MPO-derived HOCl on human plasma FN, samples of the protein were treated with either reagent HOCl (bolus addition of 0, 100, and 500 μM) or an MPO-H_2O_2-Cl^- enzymatic system with 500 μM H_2O_2. Modified and control samples were analysed by peptide mass mapping using mass spectrometry without reduction or alkylation as these interfere with the detection and quantification of some modifications, particularly chlorinations ([48]; T. Nybo, M.J. Davies, A. Rogowska-Wrzesinska, unpublished data). As no reduction step was employed, disulfide-linked peptides remain in the digestion mixture, resulting in a decreased overall coverage of the protein sequence. The disulfide-rich domains of FN (Heparin/Fibrin I, Collagen, and Fibrin II) account for the majority of the missing sequence coverage, with the total coverage being ~66% in untreated control samples (Fig. 1). In contrast, near complete coverage was obtained for the DNA-, Cell-, and Heparin II- binding domains (Fig. 1).

Treatment of FN with 100 and 500 μM HOCl resulted in the detection of multiple modifications (Table 1, Supplementary Tables 1,2), with only species detected in at least two out of three experimental treatments, and none of the controls, reported. A greater number, and a higher extent of modification, was detected with 500 μM HOCl compared to the control, or 100 μM treatment (Supplementary Figs. 1–5). Thus, with the lower oxidant dose, 6 modifications were detected at 6 different sites within the covered sequence, whereas with 500 μM HOCl, 25 modifications were observed. In some cases, multiple modifications were detected within a single peptide (e.g. at Met, M, or Tyr, Y, in the peptide: VTIMWTPPESAVTGYR), or as a result of both mono- and di-chlorination of a Tyr residue at a single site (e.g. at the first Tyr in the peptide: IYLYTLNDNAR). Three major types of modification were detected: oxidation of Met residues (3 sites: Met-926, Met-1783, Met-2050) to give an m/z + 16 species assigned to the sulfoxide, oxidation at Trp residues (5 sites: Trp-927, Trp-1195, Trp-1468, Trp-1742, Trp-1923) to give an m/z + 16 species, and mono- or di-chlorination at Tyr residues (16 sites: see Table 1). With the 100 μM treatment only monochlorination (to give 3-ClTyr) at Tyr was detected, whereas with the 500 μM dose, dichlorination to give 3,5-Cl_2Tyr was detected at two specific Tyr residues (Tyr-687 and Tyr-1882). In these cases monochlorination was detected at the lower HOCl dose, suggesting that these

Fig. 1. Coverage map obtained for human plasma FN (2.27 μM) treated with 0, 100, and 500 μM HOCl. Dark grey: detected sequence; light grey: missing sequence. Total sequence length: 2386 amino acids, with 66% coverage. Red bars indicate position of disulfide bonds. Known functional domains on the protein are indicated by boxes.

Table 1
Nature and sites of modifications induced by reagent HOCl (100 or 500 μM), or a MPO/H_2O_2/Cl^- system with 500 μM H_2O_2. Modified residue(s) are indicated in bold in the peptide sequence. Numbering is from the gene sequence with amino acids 1–31 being the signal peptide. For details of oxidant treatments, see Section 2. * and ** indicate statistically significant differences to the untreated samples at the $p < 0.05$ and $p < 0.01$ levels respectively.

Modified residue	Peptide residues	Peptide sequence(s)	Modification detected	Relative site occupancy of modifications Treatment		
				100 μM HOCl	500 μM HOCl	MPO /H_2O_2/Cl^-
Tyr-59	58–67	HY**Q**INQQWER	3-ClTyr		0.19*	
Trp-65	58–67	HYQINQQ**W**ER	Trp oxidation			0.24**
Trp-484	480–487	IGDQ**W**DK	Trp oxidation			0.15**
Tyr-666	657–669	EATIPGHLNS**Y**TIK	3-ClTyr		1.04*	
Tyr-687	673–694	PGVVYEGQLISIQQ**Y**GHQEVTR	3-ClTyr	0.14**	1.56**	0.28*
Tyr-687	673–694	PGVVYEGQLISIQQ**Y**GHQEVTR	3,5-Cl_2Tyr		0.02**	
His-689	673–694	PGVVYEGQLISIQQYG**H**QEVTR	His oxidation			0.31**
Met-926	923–938	VTI**MW**TPPESAVTGYR	Met or Trp oxidation	11.74*	40.24**	
Trp-927	923–953	VTI**MW**TPPESAVTGYRVDVIPVNLPGEHGQR				
Tyr-937	923–938	VTIMWTPPESAVTG**Y**R	3-ClTyr		0.12*	
Tyr-941	940–950	Q**Y**NVGPSVSK	3-ClTyr		1.16	0.28**
Tyr-973 / Tyr-974	959–976	NTFAEVTGLSPGVT**YY**FK	3-ClTyr	0.38**	3.05**	0.63**
Tyr-1062	1055–1070	NLQPASE**Y**TVSLVAIK	3-ClTyr		0.07*	
Trp-1195	1170–1197	VVTPLSPPTNLHLEANPDTGVLTVS**W**ER	Trp oxidation		2.56**	
Tyr-1206	1198–1207	STTPDITG**Y**R	3-ClTyr		3.30**	0.04**
Trp-1468	1452–1476	DLEVVAATPTSLLIS**W**DAPAVTVR	Trp oxidation		3.73**	
Tyr-1538	1525–1539	GDSPASSKPISIN**Y**R	3-ClTyr		0.51**	
	1533–1539	PISIN**Y**R				
Trp-1742	1730–1753	FTQVTPTSLSAQ**W**TPPNVQLTGYR	Trp oxidation		0.39**	
Tyr-1572	1562–1573	WLPSSSPVTG**Y**R	3-ClTyr		1.45**	0.02**
Met-1783	1763–1787	TGPMKEINLAPDSSSVVVSGL**M**VATK	Met oxidation	7.53**	14.48**	16.73**
	1767–1787	EINLAPDSSSVVVSGL**M**VATK				
Tyr-1788	1788–1797	**Y**EVSVYALK	3-ClTyr		1.03**	
Tyr-1793	1788–1797	YEVSV**Y**ALK	3-ClTyr		1.03**	0.14**
Trp-1923	1911–1927	FLATTPNSLLVS**W**QPPR	Trp oxidation		0.18*	
Tyr-1879	1867–1880	SYTITGLQPGTD**Y**K	3-ClTyr		0.15*	
Tyr-1882	1881–1891	I**Y**LYTLNDNAR	3-ClTyr	0.79*	6.08**	1.73**
Tyr-1882	1881–1891	I**Y**LYTLNDNAR	3,5-Cl_2Tyr		0.14**	0.06**
Met-2050	2020–2058	TPFVTHPGYDTGNGIQLPGTSGQQPSVGQQ**M**IFEEHGFR	Met oxidation		26.15**	
	2020–2059	TPFVTHPGYDTGNGIQLPGTSGQQPSVGQQ**M**IFEEHGFRR				
Tyr-2076	2071–2091	HRPRP**Y**PPNVGEEIQIGHIPR	3-ClTyr		0.64**	
Tyr-2302	2301–2310	T**Y**HVGEQWQK	3-ClTyr		0.71**	0.08**

residues are particularly prone to modification.

Treatment with the MPO-H_2O_2-Cl^- system, using 500 μM H_2O_2, also resulted in the detection of multiple modifications (Table 1). This system gives near stoichiometric conversion of H_2O_2 to HOCl, as assessed by either the MCD or TMB assays (Supplementary Fig. 6). The modifications induced by the enzyme system reproduced some, but not all, of the modifications detected with the 500 μM HOCl system. Thus, 8 of the 3-ClTyr, and 1 of the 3,5-Cl_2Tyr, sites were reproduced. For Met oxidation, one site was reproduced (Met-1783), but two Trp oxidation sites (Trp-65, Trp-484) and one His (His-689) oxidation (m/z + 16) were also detected.

In some cases, multiple modifications were detected in close proximity within particular peptides, or regions of the sequence. Thus, Fig. 2 shows the fragment ion spectra of the peptide $_{923}$VTIMWTPPESAVTGYR$_{938}$ which was detected with modifications (oxidations) at Met-926 and Trp-927, and chlorination at Tyr-937. This cluster of damage was not detected with the MPO-H_2O_2-Cl^- system. These modifications occurred both independently, producing peptide forms with each modification individually, and also as co-occurring species. The site assignment of the oxidation is determined by a + 16 Da mass shift on either fragment ion y_{12} for Trp-927 or y_{13} for Met-926. Observation of predominantly no-mass shift y_{12} and a lower abundance of the mass shifted y_{12}-ion indicate that Trp-927 is modified to some extent, but Met-926 is the primary target.

Quantification of the extent of modification at particular sites was assessed by determining the relative site occupancy (RSO). Overall, FN was modified to a lesser extent by the MPO enzymatic system when compared to the 500 μM reagent HOCl system, both in number of sites and in relative site occupancy. A number of these modifications occur in functionally-important domains (Fig. 3). Thus, oxidation of Met-1783 was detected with both 500 μM HOCl and the MPO-H_2O_2-Cl^- system, and to a lesser extent with 100 μM HOCl (Fig. 4A and C). For Tyr-1882, 3-ClTyr was observed with 100 μM HOCl, while at 500 μM HOCl further chlorination to form 3,5-Cl_2Tyr was detected, as well as significantly higher levels of 3-ClTyr (Fig. 4B and D). Interestingly, no chlorination was observed on the nearby Tyr-1884 residue. Summation of all of the relative site occupancy data for 3-ClTyr formation gives values of ~1.3, ~ 22.1 and ~ 3.2 for the 100 μM HOCl, 500 μM HOCl and MPO enzymatic systems respectively. Inclusion of all the observed modifications (i.e. chlorination at Tyr and oxidations at Met, Tyr, His and Trp) gives values of ~ 20.6, ~ 110.0 and ~ 20.7 for the 100 μM HOCl, 500 μM HOCl and MPO systems respectively.

3.2. Quantification of total 3-chlorotyrosine

The total extent of 3-ClTyr formation with reagent HOCl was determined by complete hydrolysis of the native and modified proteins by acid hydrolysis, and subsequent separation and quantification of the released 3-ClTyr by LC-MS, using an isotope-labelled product as an internal standard [47]. Under the conditions used the concentration of 3-ClTyr detected on the untreated protein was ~ 9.7 μmoles 3-ClTyr per mole protein, and ~ 0.97 mmoles 3-ClTyr per mole parent Tyr, based on the presence of 100 Tyr residues in parent FN. Treatment of the FN with 100 μM HOCl increased the 3-ClTyr levels ~ 30-fold (i.e. ~ 28.5 mmoles 3-ClTyr per mole parent Tyr), and treatment with 500 μM HOCl increased the 3-ClTyr levels 141-fold (i.e. ~ 137 mmoles 3-ClTyr per mole parent Tyr). These correspond to % conversions (after subtraction of control values) of ~ 2.8 and ~ 13.7 for 3-ClTyr formation from the

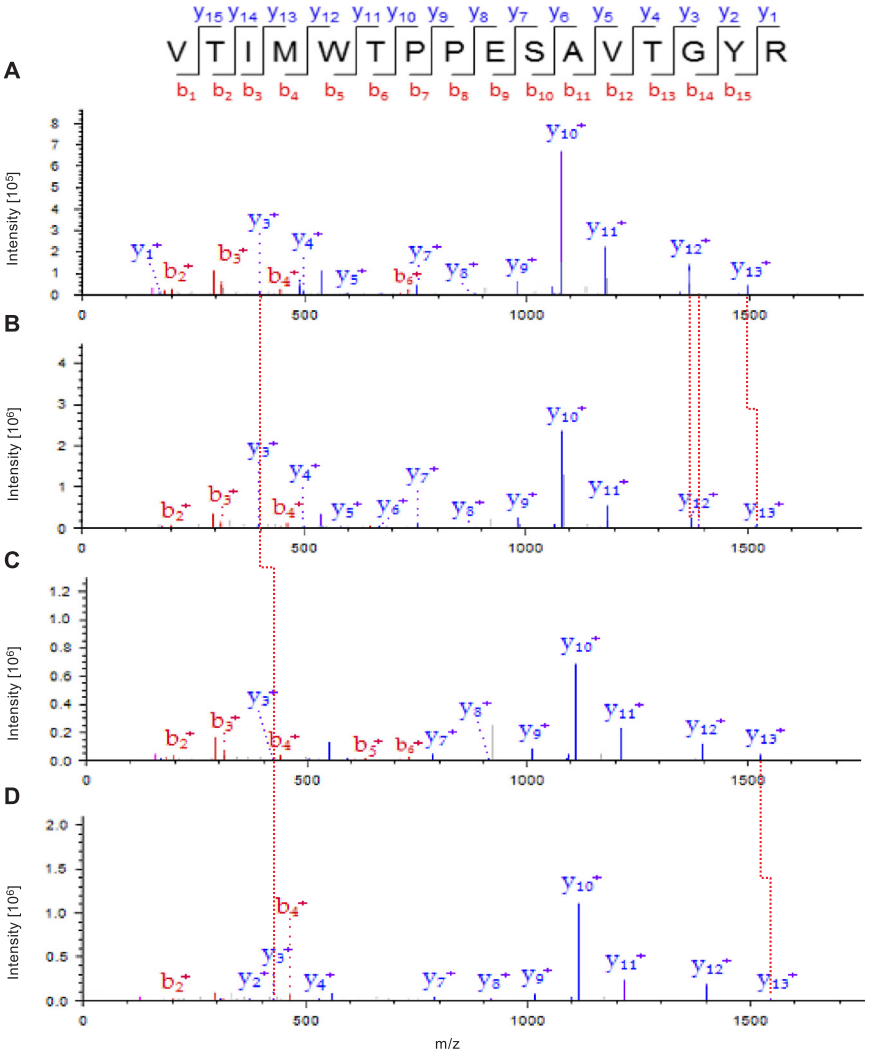

Fig. 2. Fragment ion spectra from four native and modified forms of the peptide $_{923}$VTIMWTPPESAVTGYR$_{938}$ from human plasma FN treated with 500 µM HOCl. (A) Native peptide; (B) single oxidation at Met-926 and to lesser extent at Trp-927; (C) single chlorination of Tyr-937; (D) simultaneous oxidation at Met-926 and chlorination at Tyr-937. The oxidations result in + 16 Da mass shift on ions y_{12} (for oxidation at Trp-927) and y_{13} (for oxidation at Met-926). The chlorination at Tyr-937 is indicated by the + 34 Da mass shift of the y_3 ion. These mass shifts are indicated by the red lines. For fragment ion masses see Supplementary Fig. 3.

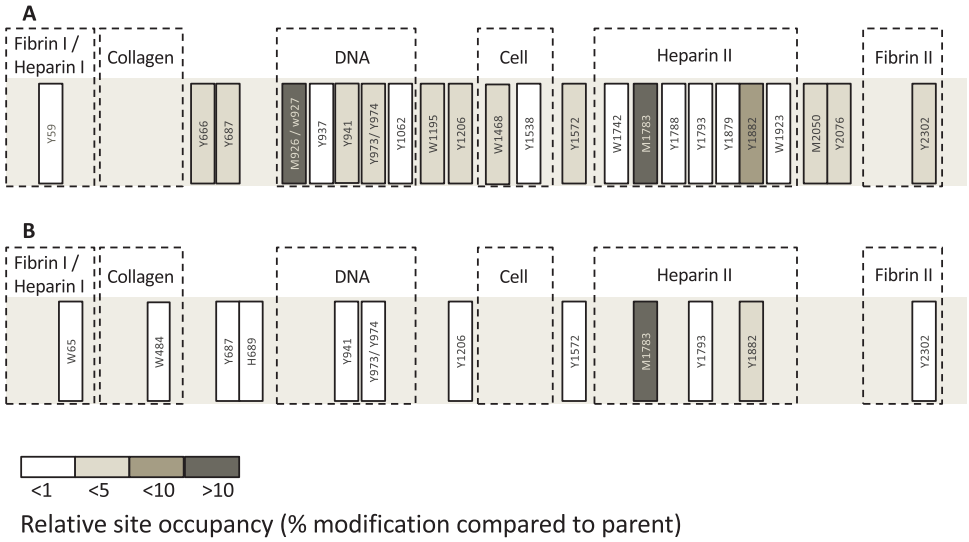

Fig. 3. Schematic of the functional domains of human plasma FN, sites of modification (Table 1) and relative site occupancies (% modification) after treatment with (A) 500 µM HOCl, or (B) exposure to MPO/H_2O_2/Cl^- with 500 µM H_2O_2. For further details, see Materials and methods. M = Met, H = His, W = Trp, Y = Tyr. Modifications (m/z + 16) detected at M, H, W are assigned to mono-oxidation. Modifications at Y were single or double chlorinations to give 3-ClTyr or 3,5-Cl_2Tyr.

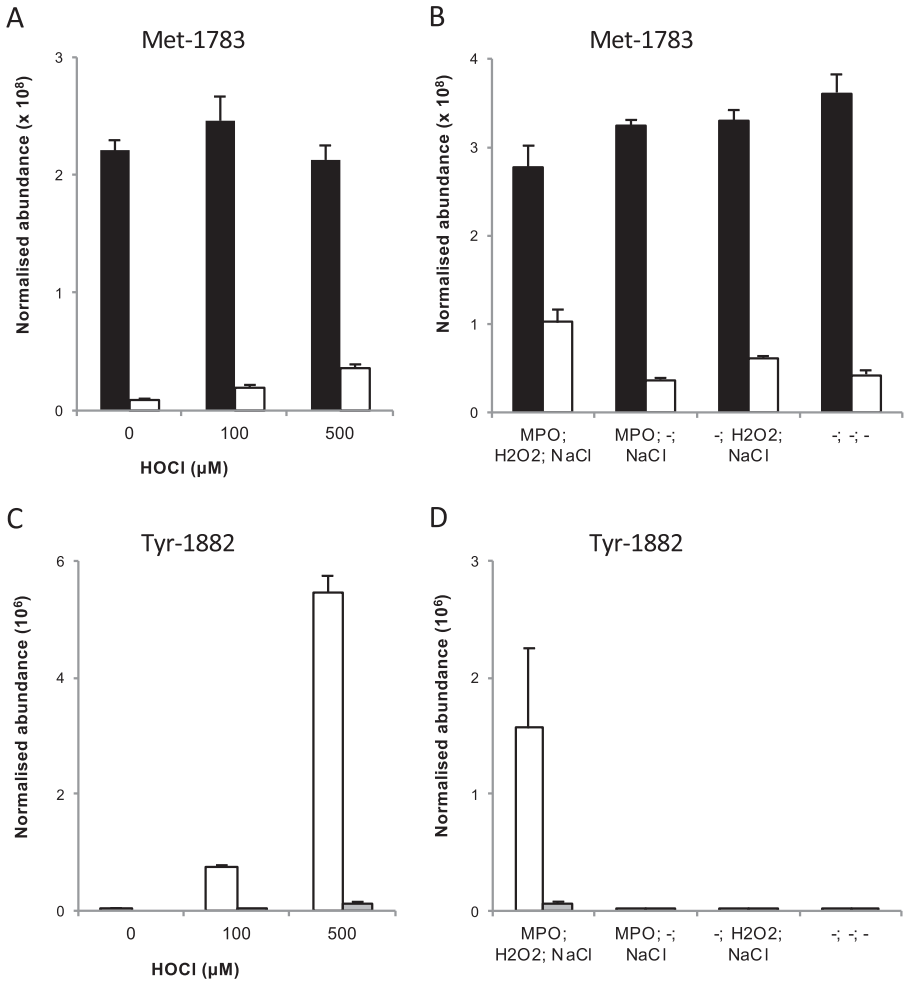

Fig. 4. Plots of normalised abundance (± standard errors), calculated from peptide precursor extracted ion chromatograms from FN after treatment with 0, 100, and 500 μM HOCl for (A) Met-1783 and (C) Tyr-1882, or a MPO/H_2O_2/Cl^- system for (B) Met-1783 and (D) Tyr-1882. Black bars = native untreated samples, white bars = singly modified peptides, grey bars = doubly modified peptides. Met-1783 was identified in the peptide $_{1767}$EINLAPDSSSVVVSGLMVATK$_{1787}$, and Tyr-1882 in the peptide $_{1881}$IYLYTLNDNAR$_{1891}$ (Table 1). For further details, see Materials and methods.

total Tyr population present in the FN sequence, by 100 and 500 μM HOCl respectively (cf. the values of ~1.3 and ~22.1 described above for the more limited number of Tyr residues detected in the FN sequence by mass spectrometry).

3.3. Increased heparin affinity of HOCl-modified FN

As modifications were detected as residues within FN functional domains (Fig. 3), further analyses were carried out to examine the potential importance of these modifications. As multiple modifications (Trp-1742, Met-1783, Tyr-1788, Tyr-1793, Tyr-1879, Tyr-1882, Trp-1923) were detected within the Heparin-II domain (residues 1721–1991), the impact of these modifications on the ability of FN to bind heparin was determined by heparin affinity chromatography (Fig. 5). The elution time of native FN (8.13 min) was significantly shorter from those for FN pre-treated with 100 μM HOCl (8.2 min) or 500 μM HOCl (8.32 min) (Fig. 5), consistent with a stronger binding of the modified FN to the heparin molecules present in the column.

3.4. Fibronectin modified by HOCl or a MPO-H_2O_2-Cl^- system gives rise to altered adhesion and proliferation of primary human coronary artery smooth muscle cells (HCASMC)

To examine the impact of oxidant-induced changes on FN, studies were carried out in which pure cultures of primary human coronary artery smooth muscle cells (HCASMC) were added to tissue culture plates containing native or pre-modified FN. Thus, HCASMC were incubated on native or HOCl-modified FN for 90 min at 37 °C in a cell incubator before removal of non-adherent cells by washing, and subsequent staining with trypan blue and examination by bright field microscopy (Fig. 6A, top row). Alternatively, cells were added to FN-coated glass culture slides that had been pre-exposed to HOCl (20 or 100 μM) for 2 h at 37 °C. The adherent HCASMC were then visualized by staining for F-actin and the nucleus, and fluorescence microscopy (Fig. 6A, bottom row). The HCASMC showed a characteristic spread spindle shape on native FN, but were less spread and were typically "rounded up" on HOCl-treated FN, indicative of poor adherence to oxidized FN. Quantification of cell adherence was carried out using HCASMC, pre-loaded with the fluorescent dye Calcein-AM, incubated on native or HOCl-modified FN (90 mins, 37 °C), non-adherent cells removed by washing, and quantification of the number of adherent cell by fluorescence. Using this approach, and with native FN taken as 100%, a statistically-significant decrease in cell adherence was detected on pre-treatment of the FN with 10 μM or greater concentrations of HOCl, with this occurring in a dose-dependent manner (Fig. 6B).

Experiments with an MPO-H_2O_2-Cl^- system with 20 nM MPO, 200 mM Cl^- and varying amounts of H_2O_2, reproduced the effects of reagent HOCl. Thus, pre-treatment of FN with the enzyme system decreased HCASMC adhesion to the modified FN, relative to native FN, with this occurring in a dose-dependent manner with increasing H_2O_2

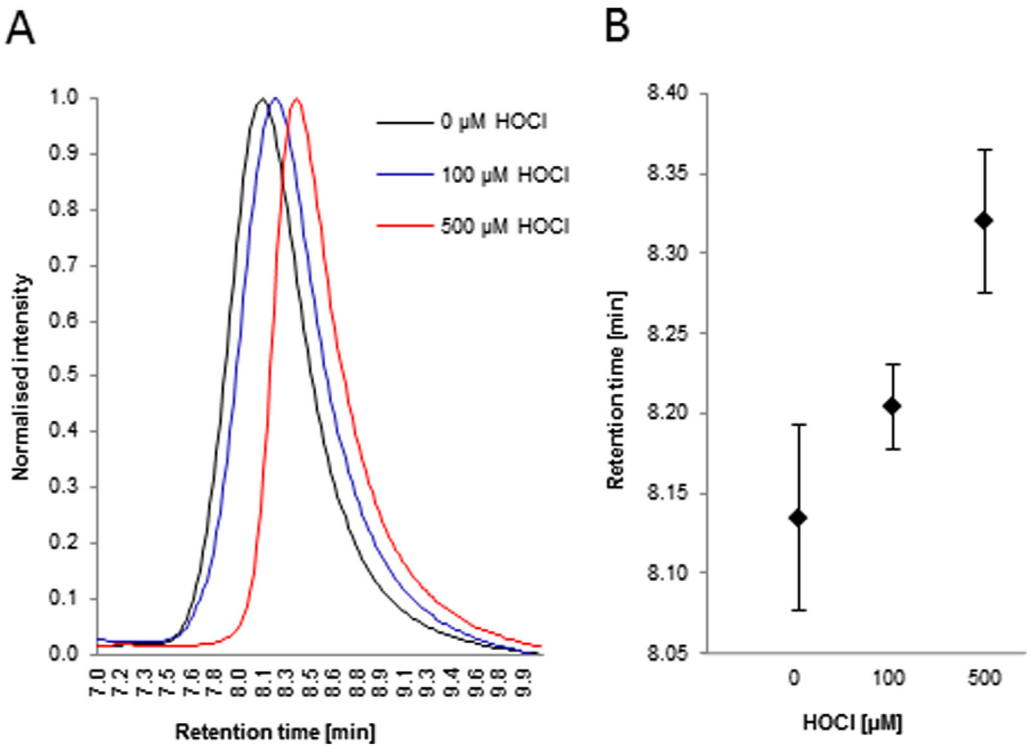

Fig. 5. Heparin-affinity chromatography of human plasma FN (2.27 μM), either native (no HOCl treatment), or after modification with 100 or 500 μM HOCl. The peaks in (A) were normalised to equal intensity, and are representative data. (B) Plot of mean elution times (± standard errors) from 3 independent experiments. Black line: native FN; blue line: treatment with 100 μM HOCl; red line: treatment with 500 μM HOCl. For further details, see Materials and methods.

concentrations, with statistical differences detected at 1 μM or greater concentrations of H_2O_2 (Fig. 6C).

Further studies examined the subsequent proliferation of HCASMC adhered to the native and modified FN. In these experiments, the cells were allowed to adhere to the native or HOCl-modified FN (pre-treated with 1 μM HOCl to ensure significant numbers of adherent cells), and then allowed to proliferate for 48 h in standard growth medium. After this period, the number of metabolically active cells was determined using the MTS assay. Due to the differing initial numbers of cells at the beginning of the proliferation phase (see data above), the data were corrected for this parameter by plotting the fluorescence intensity at day zero against the values obtained from the MTS assay at day 2. The resulting data (Fig. 7A) show that the gradient of the plots for the oxidant-modified FN were greater than that for the native FN (red dots versus blue dots) indicating that the cells proliferated more rapidly on the oxidant-treated FN. These data are quantified in Fig. 7B as a normalised proliferation rate.

3.5. *Fibronectin modified by HOCl or a MPO-H_2O_2-Cl^- system gives rise to altered gene expression in human coronary artery smooth muscle cells (HCASMC)*

As the data presented above are consistent with decreased adherence, but a subsequent increased rate of HCASMC growth, on oxidant-modified FN, the expression of a number of mitosis-related genes were examined in the HCASMC cultured on native versus HOCl-treated FN. mRNA was collected from cells incubated on the native and modified FN at day 2 after adhesion (see preceding section) and analysed for the fold-change in PCNA (Proliferating Cell Nuclear Antigen), CCNA 1 (Cyclin-A1) and CCNB 1 (Cyclin-B1) by RT-PCR with β-actin used as a housekeeping gene. Significantly-elevated levels of these genes were detected for the cells exposed to the FN pre-treated with all three concentrations of HOCl examined (1, 10 and 50 μM), compared to native FN, with the greatest increases (~ 4.7-fold) seen for PCNA after treatment of the FN with 1 μM HOCl (Fig. 8). Lower, but significantly-elevated expression (~ 3-fold) was detected with higher HOCl concentrations. An approximate doubling of the expression of CCNA 1 and CCNB 1 was seen with all of the FN samples pre-treated with the different HOCl concentrations, with no statistical differences detected between the different concentrations (Fig. 8).

In addition to changes in mitosis-related genes, potential changes in the expression of inflammation, ECM proteins and ECM-modifying enzymes (matrix metalloproteinases, MMPs, and tissue inhibitor of matrix metalloproteinases 2, TIMP2) were examined for the cells exposed to the HOCl-modified FN (as above) compared to native FN. The resulting data is shown as a heat map relative to the native FN data on a log scale in Fig. 9.

Exposure of the cells to FN modified with different concentrations of HOCl (1 μM, 10 μM, 50 μM), compared to native FN, resulted in increased mRNA expression of *IL-6* ($P < 0.05$), with this mirrored by a small, but significant, increase in the level of IL-6 protein, detected by ELISA, in the conditioned cell media from the cultured HCASMC (Supplementary Fig. 7), with this occurring in a dose-dependent manner with increasing HOCl-exposure of the FN. The mRNA levels of *iNOS* were also significantly elevated ($P < 0.05$) at all HOCl-concentrations tested, whereas only small changes were detected with *IL-1β* and *COX-2* (Fig. 9).

Gene expression for multiple ECM proteins, including *FN* and *LAMA1* were significantly up-regulated ($P < 0.05$), while the expression of *LAMB2* was markedly down-regulated ($P < 0.05$), with these changes being more marked at the higher concentrations of HOCl (10 and 50 μM) (Fig. 9). Less marked changes were detected in the mRNA levels of the other matrix proteins examined (Fig. 9). Significant up-regulation of mRNA of a number of MMPs known to be involved in ECM remodelling, was also detected (Fig. 9). Significant increases were detected, particularly for *MMP8*, *MMP11* and *MMP13*, for HCASMC incubated on FN modified with 10 μM and 50 μM HOCl, with this extending down to the 1 μM HOCl treatment for *MMPs 11* and *13*. These data are consistent with a range of cellular responses including increased expression of new matrix proteins, and an attempted remodelling of the ECM surrounding the cells in response to oxidant-mediated changes to the FN to which the cells are attached.

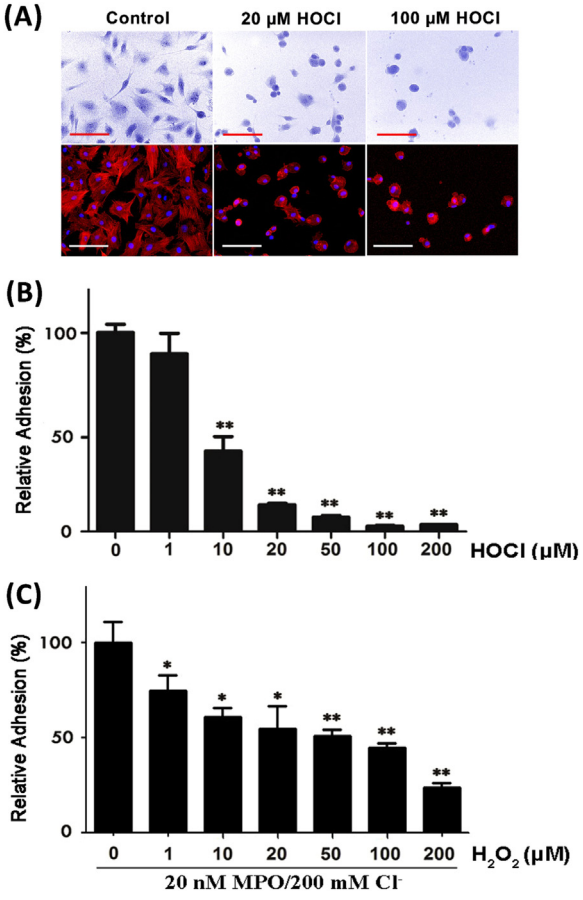

Fig. 6. Effect of pre-treatment of FN with HOCl (panels A, B) or MPO/H_2O_2/Cl^- with the indicated concentrations of H_2O_2 (panel C), on subsequent adhesion of primary human coronary artery smooth muscle cells (HCASMC). Panel (A), top row: HCASMC incubated with trypan blue imaged at 20-fold magnification using bright field microscopy. Panel (A), bottom row: Adherent cells on native or HOCl-treated FN stained for F-actin fibres and nuclei and imaged using fluorescence microscopy. Panels (B, C), Quantification of adhewrent HCASMC pre-loaded with 5 μM calcein AM with subsequent fluorescence detection. For further details see Materials and methods.

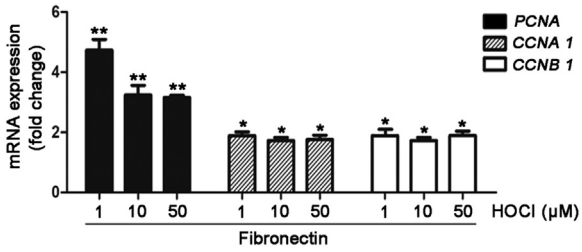

Fig. 8. Effect of HOCl-treated FN, compared to parent FN, on mRNA expression of mitosis-related genes in HCASMC. HCASMC were incubated on native or HOCl-treated (1, 10 or 50 μM HOCl) fibronectin in 24-well plates for 48 h (as described in the legend to Fig. 7) before RNA was extracted for cDNA synthesis and real time PCR. For further details, see Materials and methods.

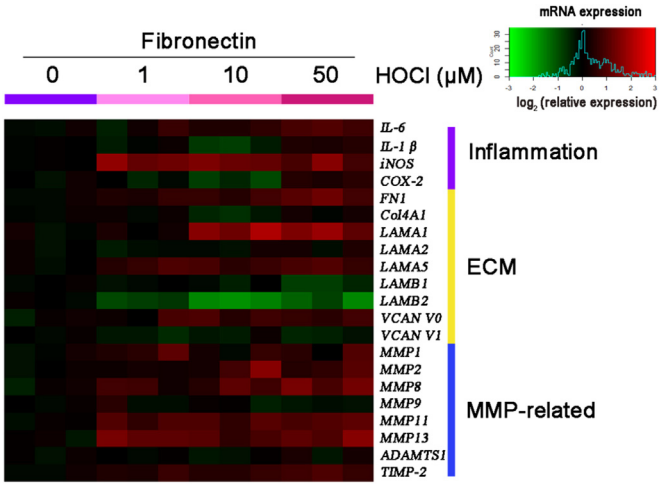

Fig. 9. Effect of HOCl-treated FN (1, 10 or 50 μM HOCl), compared to parent FN, on mRNA expression of mitosis-related genes in HCASMC. HCASMC were incubated on native or HOCl-treated fibronectin for 48 h before RNA extraction, cDNA synthesis and real time PCR. The heat map indicates changes in expression on a log scale with green colouration indicating down-regulation, and red colouration indicating up-regulation. The genes examined include those involved in inflammation (purple), extracellular matrix proteins (ECM, yellow) and matrix metalloproteinases (MMP) and a MMP inhibitor (TIMP-2) (MMP-related: blue). For further information see main text and Materials and methods.

4. Discussion

In this study, we have identified and quantified sites of oxidation and chlorination on the major extracellular matrix protein fibronectin (FN), induced by the inflammatory oxidant HOCl, when added as a reagent, or generated by a MPO-H_2O_2-Cl^- enzyme system. The plasma form of FN plays a key role in the early physiological responses to tissue injury as it binds to fibrin and is a component of blood clots [3]. The fibrin-FN network is critical to the adhesion, migration and proliferation of fibroblast and endothelial cells and therefore tissue repair,

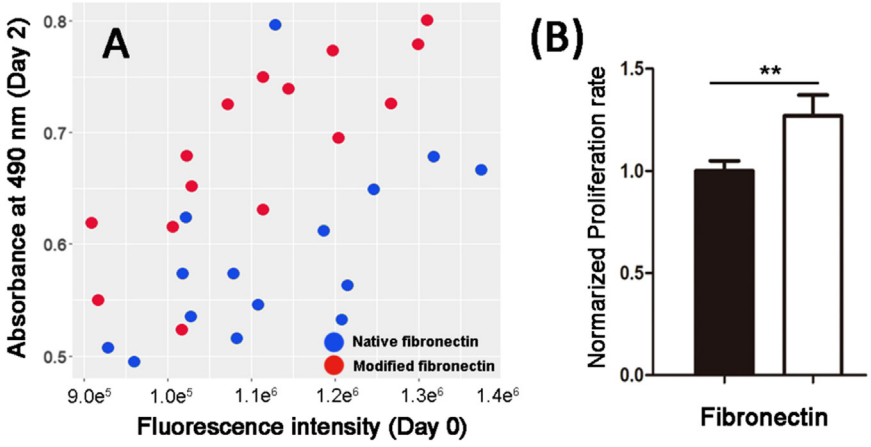

Fig. 7. Effect of pre-treatment of FN with reagent HOCl (1 μM) on subsequent proliferation of adherent primary human coronary artery smooth muscle cells (HCASMC). Panel (A), HCASMC (pre-loaded with 5 μM calcein AM) were added to untreated FN, or FN pre-treated with 1 μM HOCl and washed to remove excess oxidant. Adherent cells were quantified by fluorescence. The cells were then incubated for 48 h in growth medium and the final cell population determined by MTS assay. (B) The proliferation rate of HCASMC for both groups displayed as the ratio of normalised cell populations at 0 and 48 h. For further details, see Materials and methods.

including within the artery wall [4,5]. FN is present in the arterial wall under normal physiological conditions [7], but increased concentrations, and altered isoforms, are present in atherosclerotic lesions [8] with this changing during lesion development [9]. Increased lesion FN levels are mirrored by increases in plasma FN in people with coronary artery disease [10], with this ascribed to remodelling of the damaged vascular wall and ECM deposition in the fibrous caps of lesions [11]. The extent of such ECM deposition has been reported to be a critical factor in lesion stability and propensity to rupture, and therefore the occurrence of heart attacks and strokes [11]. Previous studies have provided data consistent with damage to, and destabilization of, components of atherosclerotic plaques by oxidants generated by inflammatory cells [17,18], with oxidant-mediated damage detected on ECM perlecan [49,50], laminin [51], (tropo)elastin [52] and fibronectin [53] in human atherosclerotic lesions, as well as lesion lipoproteins (e.g. [36,37,39,54]). Evidence has been presented a role for both peroxynitrous acid (ONOOH, from reaction of $O_2^{\bullet-}$ with $NO^{\bullet}$; reviewed [55]) as well as MPO-derived HOCl [29,56,57].

Despite the reported importance of ECM damage and lesion destabilization by oxidants, there is limited information on the modifications induced by HOCl on isolated FN, or FN in the arterial wall, though it is well established that FN is a target for HOCl [26–28,57]. There is however, considerable evidence for the presence of elevated and enzymatically active MPO in human atherosclerotic lesions, with this being localized in regions prone to rupture [23], and modified FN co-localizes with MPO in human atherosclerotic lesions [29]. Elevated MPO levels have been reported, in a large number of studies, to be both diagnostic and prognostic of major adverse cardiovascular events (e.g. [25,58–63]).

In addition to altering the composition and structure of FN, oxidant-damage may also affect FN function, particularly with regard to ECM assembly, due to the key role that this protein plays in interacting with other matrix proteins (cf. the fibrin, heparin, and collagen-binding sites on FN). FN modifications may also affect cell-ECM interactions due to the presence of a both a cell binding (RGD) site which interacts with cellular integrin (α5β1) proteins, and a binding site for vascular endothelial growth factor (VEGF) within the Hep II binding site (in the III_{13} and III_{14} modules) which plays a key role in endothelial cell migration and proliferation [1]. Recent studies have shown that primary human coronary artery endothelial cells (HCAEC) show decreased adhesion and proliferation on FN modified by both HOCl and a MPO-H_2O_2-Cl^- enzyme system, with this being associated with damage to specific FN epitopes including the cell-binding region [57].

HOCl preferentially targets sulfur-containing amino acids (Cys, Met and cystine) [22,30,31], but can also modify His, Trp, Lys and Tyr residues to a significant extent [22]. The formation of 3Cl-Tyr from reaction with Tyr residues has been used to elucidate the role of MPO and HOCl in tissue damage as this product is a stable, distinctive and well-established biomarker of HOCl-mediated damage [34–36].

The data presented here indicates that both reagent HOCl and the MPO-H_2O_2-Cl^- system can generate significant, but selective, damage on FN, and that these changes induce significant functional alterations with regard to smooth muscle cell adhesion, proliferation, gene expression and phenotype. The enzyme system was provided with 500 μM H_2O_2 in order to generate ~ 500 μM HOCl to allow direct comparison between the reagent and enzyme systems, and hence any potential localization or other effects induced by the enzyme.

Of the residues expected to react with HOCl and MPO-H_2O_2-Cl^- system [22,30,64], a high proportion were present in the peptide sequences detected by the MS mapping. Of the 26 Met residues present in the human plasma FN sequence (UniProt – P02751), 14 were observed by MS, with 27 of 39 detected for Trp, 33 from 55 for His, and 64 from 100 for Tyr. Of these residues only 3 Met, 7 Trp, 1 His and 16 Tyr residues were detected as targets for oxidation (in the case of Met, Trp and His) or chlorination (Tyr), when exposed to reagent HOCl (100 or 500 μM) or the MPO-H_2O_2-Cl^- system. This corresponds to modification levels of ~11.5, ~12.8, ~2.0 and ~15.0% for Met, Trp, His and Tyr respectively when considered as a % of the full sequence total, and ~21.4, ~25.9, ~3.0 and ~23.4%, respectively, of the Met, Trp, His and Tyr residues detected. The similarity of these percentages for Met, Trp and Tyr, suggest that factors other than the absolute reactivity of a particular type of residue with HOCl (which decreases in the order Met > > Trp > Tyr; [22,30,64]) must play a role in determining which sites are modified.

Summation of the extents of 3-ClTyr formation detected by both MS and the amino acid analyses, indicates that between 13% and 22% of the Tyr residues are modified by 500 μM HOCl, and hence ~ 1 in 5 FN molecules contains a 3Cl-Tyr residue after this treatment. The *overall* extent of modification (i.e. including oxidation) was considerably higher (primarily driven by the high extent of Met modification), with ~ 1 in 5 FN molecules carrying a modification after treatment with 100 μM HOCl or the MPO system, and all (~ 110%) FN molecules, on average, containing a single modification after treatment with 500 μM HOCl.

These site occupancy data indicate that only a subset of the residues detected by MS are detected in a modified form, and hence it is likely that some residues are much more susceptible to modification than others. Therefore, as the sequence coverage was only ~ 66%, there may be modifications to significantly more residues within the non-detected portions of the sequence. However the relative similarity of the data between the MS and total amino acid analyses suggest that a reasonably similar extent of modification must also be occurring in the non-observed regions of the sequence. Most of the "missing" sequence is comprised of the cystine (disulfide)-rich Hep I/Fibrin I, Collagen, and Fibrin II domains of FN. These regions are difficult to detect using the current protocol as a result of the absence of a reduction and alkylation steps which remove the disulfide bonds and thereby release these peptides. This protocol was however employed as reduction and alkylation have been shown to cause artefactual loss of modification sites ([48]; T. Nybo, M.J. Davies, A. Rogowska-Wrzesinska, unpublished data).

Comparison of the data obtained with 500 μM HOCl and the MPO system shows a similar pattern of chlorination but fewer sites, and lower extents, of modification, with only 8 of the 16 Tyr chlorinations seen with HOCl, reproduced by the MPO system. Oxidation was observed at 4 residues with the enzyme system (2 × Trp, 1 × His, 1 × Met) compared to 7 with HOCl, though the position and nature of the residues affected were significantly different for the oxidized residues when compared to the chlorination sites (Table 1). These findings indicate that there are differences in the *selectivity* of damage between reagent HOCl and the enzyme system with regard to the susceptibility of certain sites to modification. The overall extent of modification was also lower for the MPO system than reagent HOCl; this is perhaps understandable due to the presence of additional protein in the enzyme system (in the form of the MPO), which will also be a target for HOCl. Indeed, a number of MPO-derived peptides containing oxidation sites were detected in the enzyme experiments, though these were not analysed in detail (Nybo et al., unpublished data).

The reasons for the (apparent) altered specificity of damage observed with the enzyme system is unclear. The majority of the differences are present in the N-terminal portion of FN, which appears to be exclusively modified by the MPO-system, with this possibly due to association of the enzyme with one or more domains within this part of FN. Thus, oxidation of Trp-65 and Trp-484 were detected in the I_1 and I_7, modules, while oxidation at His-689 was also detected in module III_1. Furthermore, the absence of significant modification of Met-926 by the MPO system, which is significantly modified by reagent HOCl, is consistent with an altered conformation or accessibility of this residue in the presence of MPO, compared to its absence. It has been reported previously that MPO binds to FN [65], though MPO activity was reported to increase after binding to FN in cell-derived ECM [65,66], and the exact site of interaction has not been established. Our observations

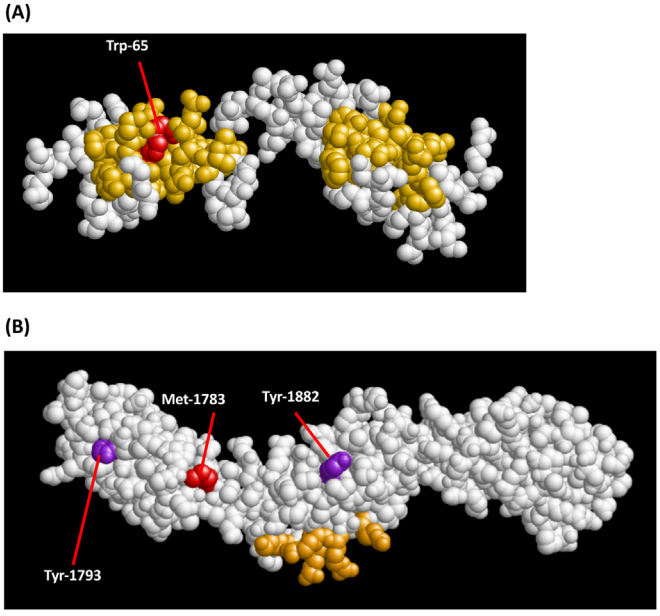

Fig. 10. Rendering of partial crystal structures of the Heparin/Fibrin I (PDB: 1O9A; top panel) and Heparin II (PDB: 1NFH; bottom panel) binding domains of FN from the corresponding PDB data files. Residues determined as being modified by the MPO-enzyme system are indicated (red = oxidized, purple = chlorinated). The residues involved in fibrin-binding in 1O9A [67] and heparin-binding in 1NFH are indicated in yellow [71].

implicate the N-terminal region.

The MPO-specific oxidation site, Trp-65, is located in loop 1 within the fibrin binding site [67] (Fig. 10). This observation is of potential significance, as a previous study has shown that chemical modification of Trp residues in this domain caused a 90% loss of heparin binding compared to unmodified controls [68]. Binding of fibrin/fibrinogen plays a key role in thrombus formation important in wound healing and stabilisation of atherosclerotic lesions [16,69,70].

For both the reagent and enzymatic systems, the Hep II domain was heavily modified with two major targets and other lesser sites of modification. The most heavily modified sites (Met-1783, detected as a $+16\,m/z$ species; and Tyr-1882, detected as both a mono- and di-chlorinated species) are surface exposed in a partial crystal structure of this domain (Fig. 10) [71]. These alterations appear to induce a higher binding affinity of the modified FN towards heparin than the unmodified form, as judged by the increased retention on the heparin column.

Cell adhesion to FN is mediated, at least in part, via interactions with cell-surface integrins, and particularly α5β1, with the RGD motif present in the cell-binding domain (module III_{10}) [72]. This interaction appears to be only sufficient for attachment and spreading of the cells, with additional interactions and signalling involving syndecan-4 required for focal adhesion formation, and the arrangement of the actin cytoskeleton into bundled stress fibres [73,74]. The signalling induced by these focal adhesions is a prerequisite for gene expression, cell cycle regulation, and control of apoptosis [75]. Syndecan-4 interacts with the Hep II domain of FN through heparin sulfate chains with specific properties [76], and activates protein kinase C-α signalling [77] in the presence of inositol phospholipids (reviewed [78,79]). Recent data also indicates that the Hep II domain is a binding domain for vascular endothelial cell growth factor (VEGF), and that bound VEGF "talks" to the cell-binding domain, with both domains required for cell adherence, proliferation and migration of endothelial cells and osteoblasts [80,81].

In the current studies, two modifications were detected in the cell-binding domain (Trp-1468, Tyr-1538) with 500 μM HOCl. Both residues are distant (within the sequence) from the RGD site (residues 1524–1526), and are modified to only a moderate (Trp-1468) or low extent (Tyr-1538). It is therefore impossible to determine whether these modifications are responsible, possibly via remotely-induced conformational changes, for the decreased HCASMC adherence observed in the current study. However, it is possible that these alterations, in conjunction with those in the Hep II region, may be sufficient to explain the observed decrease in cell adhesion.

The enhanced proliferation and altered gene expression detected for the HCASMC after initial adherence may also arise from the modifications in the Hep II domain, as this domain modulates cell signalling and cell cycle control [75]. The increased expression in PCNA, CCNA 1 and CCNB 1 in HCASMC exposed to HOCl-modified FN is consistent with the enhanced rate of cell growth detected for cells on modified compared to control FN. Modified FN also induced alterations in the expression of genes associated with ECM synthesis and remodelling, with upregulation of some matrix proteins (e.g. LAMA1), a decrease in others (e.g. LAMB2), and upregulation of the expression of multiple MMPs. Increased expression of inflammatory genes, and particularly iNOS and IL-6, were also detected, with higher expression of the latter reflected in increased IL-6 protein excretion. Together these data suggest that modified FN generates phenotypic changes in adherent HCASMC with these having proliferative and pro-inflammatory characteristics.

These changes are of potential biological significance as it is well established that during the development of atherosclerotic lesions, medial smooth muscle cells switch from a quiescent contractile phenotype to a migratory and proliferative form. The latter migrate into the growing lesion, aided via a disruption of the elastic lamina (arising from either direct oxidation or MMP-mediated), and play an important role in generating the fibrous cap of the lesion via ECM synthesis. The assembly of newly-synthesized ECM by such cells may also be of critical importance, as highly fibrous lesions are less prone to rupture and thrombus formation. In this respect, it is interesting to note that one of the other modifications detected, at Tyr-666 (observed as 3-ClTyr) in the anastellin domain, is critical to superfibronectin formation and fibril assembly [1]. Mutation of this Tyr, together with Leu-663 to Ala, abolishes polymerization activity [82], without affecting FN secondary structure, fibronectin binding, or p38 kinase activation [82,83]. It is therefore possible that the synthesis and assembly of new FN fibres by HCASMC, in the presence of HOCl-modified FN, may be incomplete or modulated as a result of the Tyr-666 chlorination. Altered FN fibre assembly may have downstream consequences, as correct FN fibrillogenesis is a requirement for the correct deposition of other ECM materials including fibrillin-1 microfibrils [84] and collagen-containing structures [85]. The modifications to FN may therefore result in a weakened or modified ECM structure in lesions.

Overall, these data provide novel insights into how damage induced by MPO and its oxidants, can change the ECM environment and have consequent effects on associated cells. Using MS-based quantification of site-specific amino acid modifications we have shown that MPO-generated HOCl modifies selected regions in FN, with damage observed in functional domains, including damage clusters within the heparin-binding sequence. The modified FN exhibits increased binding affinity for heparin. Human coronary artery smooth muscle cells (HCASMC) show decreased adherence, increased proliferation and growth, and altered gene expression in response to modified FN, with increased expression of genes involved in ECM formation and remodelling. These findings indicate that modified FN may play a major role in the formation, development and stabilisation of fibrous caps in atherosclerotic lesions.

Acknowledgements

The authors are grateful to the Novo Nordisk Foundation (Grant: NNF13OC0004294) and the Danish Council for Independent Research (Det Frie Forskningsråd, Grant: DFF-7014-00047) for financial support. ARW was supported by Independent Research Fund Denmark – Natural

Sciences (FNU) and VILLUM Foundation grant to the VILLUM Center for Bioanalytical Sciences at SDU.

Appendix A. Supplementary material

Supplementary data associated with this article can be found in the online version at doi:10.1016/j.redox.2018.09.005.

References

[1] P. Singh, C. Carraher, J.E. Schwarzbauer, Assembly of fibronectin extracellular matrix, Annu. Rev. Cell Dev. Biol. 26 (2010) 397–419.
[2] R. Hynes, Molecular biology of fibronectin, Annu. Rev. Cell Biol. 1 (1985) 67–90.
[3] R. Pankov, K.M. Yamada, Fibronectin at a glance, J. Cell Sci. 115 (2002) 3861–3863.
[4] K.S. Midwood, L.V. Williams, J.E. Schwarzbauer, Tissue repair and the dynamics of the extracellular matrix, Int. J. Biochem. Cell Biol. 36 (2004) 1031–1037.
[5] W.S. To, K.S. Midwood, Plasma and cellular fibronectin: distinct and independent functions during tissue repair, Fibrogenes. Tissue Repair 4 (2011) 21.
[6] E.S. White, A.F. Muro, Fibronectin splice variants: understanding their multiple roles in health and disease using engineered mouse models, IUBMB Life 63 (2011) 538–546.
[7] S. Stenman, A. Vaheri, Distribution of a major connective tissue protein, fibronectin, in normal human tissues, J. Exp. Med. 147 (1978) 1054–1064.
[8] M.K. Magnusson, D.F. Mosher, Fibronectin: structure, assembly, and cardiovascular implications, Arterioscler. Thromb. Vasc. Biol. 18 (1998) 1363–1370.
[9] S. Stenman, K. Vonsmitten, A. Vaheri, Fibronectin and atherosclerosis, Acta Med. Scand. (1980) 165–170.
[10] K.S. Song, H.K. Kim, W. Shim, S.H. Jee, Plasma fibronectin levels in ischemic heart disease, Atherosclerosis 154 (2001) 449–453.
[11] M.J. Davies, A.C. Thomas, Plaque fissuring - the cause of acute myocardial infarction, sudden ischaemic death and crescendo angina, Br. Heart J. 53 (1985) 363–373.
[12] A. Fortuno, G. San Jose, M.U. Moreno, J. Diez, G. Zalba, Oxidative stress and vascular remodelling, Exp. Physiol. 90 (2005) 457–462.
[13] A.J. Lusis, Atherosclerosis, Nature 407 (2000) 233–241.
[14] E. Falk, P.K. Shah, V. Fuster, Coronary plaque disruption, Circulation 92 (1995) 657–671.
[15] A.C. van der Wal, A.E. Becker, C.M. van der Loos, P.K. Das, Site of intimal rupture or erosion of thrombosed coronary atherosclerotic plaques is characterized by an inflammatory process irrespective of the dominant plaque morphology, Circulation 89 (1994) 36–44.
[16] I. Rohwedder, E. Montanez, K. Beckmann, E. Bengtsson, P. Duner, J. Nilsson, O. Soehnlein, R. Fassler, Plasma fibronectin deficiency impedes atherosclerosis progression and fibrous cap formation, EMBO Mol. Med. 4 (2012) 564–576.
[17] M.D. Rees, E.C. Kennett, J.M. Whitelock, M.J. Davies, Oxidative damage to extracellular matrix and its role in human pathologies, Free Radic. Biol. Med. 44 (2008) 1973–2001.
[18] C.Y. Chuang, G. Degendorfer, A. Hammer, J.M. Whitelock, E. Malle, M.J. Davies, Oxidation modifies the structure and function of the extracellular matrix generated by human coronary artery endothelial cells, Biochem J. 459 (2014) 313–322.
[19] B. Halliwell, J.M.C. Gutteridge, Free Radicals In Biology & Medicine, Oxford University Press, Oxford, 2015.
[20] C.C. Winterbourn, A.J. Kettle, M.B. Hampton, Reactive oxygen species and neutrophil function, Annu. Rev. Biochem. 85 (2016) 765–792.
[21] M.J. Davies, C.L. Hawkins, D.I. Pattison, M.D. Rees, Mammalian heme peroxidases: from molecular mechanisms to health implications, Antioxid. Redox Signal. 10 (2008) 1199–1234.
[22] D.I. Pattison, M.J. Davies, Absolute rate constants for the reaction of hypochlorous acid with protein side chains and peptide bonds, Chem. Res. Toxicol. 14 (2001) 1453–1464.
[23] A. Daugherty, J.L. Dunn, D.L. Rateri, J.W. Heinecke, Myeloperoxidase, a catalyst for lipoprotein oxidation, is expressed in human atherosclerotic lesions, J. Clin. Investig. 94 (1994) 437–444.
[24] S.J. Nicholls, S.L. Hazen, Myeloperoxidase and cardiovascular disease, Arterioscler. Thromb. Vasc. Biol. 25 (2005) 1102–1111.
[25] W.H. Tang, Y. Wu, S.J. Nicholls, S.L. Hazen, Plasma myeloperoxidase predicts incident cardiovascular risks in stable patients undergoing medical management for coronary artery disease, Clin. Chem. 57 (2011) 33–39.
[26] M.C. Vissers, C.C. Winterbourn, J.S. Hunt, Degradation of glomerular basement membrane by human neutrophils in vitro, Biochim. Biophys. Acta 804 (1984) 154–160.
[27] M.C.M. Vissers, C.C. Winterbourn, Oxidative damage to fibronectin. 1. The effects of the neutrophil myeloperoxidase system and hocl, Arch. Biochem. Biophys. 285 (1991) 53–59.
[28] M.C.M. Vissers, C. Thomas, Hypochlorous acid disrupts the adhesive properties of subendothelial matrix, Free Radic. Biol. Med. 23 (1997) 401–411.
[29] S. Baldus, J.P. Eiserich, M.L. Brennan, R.M. Jackson, C.B. Alexander, B.A. Freeman, Spatial mapping of pulmonary and vascular nitrotyrosine reveals the pivotal role of myeloperoxidase as a catalyst for tyrosine nitration in inflammatory diseases, Free Radic. Biol. Med. 33 (2002) 1010–1019.
[30] C. Storkey, M.J. Davies, D.I. Pattison, Reevaluation of the rate constants for the reaction of hypochlorous acid (hocl) with cysteine, methionine, and peptide derivatives using a new competition kinetic approach, Free Radic. Biol. Med. 73 (2014) 60–66.
[31] M. Karimi, M.T. Ignasiak, B. Chan, A.K. Croft, L. Radom, C.H. Schiesser, D.I. Pattison, M.J. Davies, Reactivity of disulfide bonds is markedly affected by structure and environment: implications for protein modification and stability, Sci. Rep. 6 (2016) 38572.
[32] C.L. Hawkins, M.J. Davies, Hypochlorite-induced damage to proteins: formation of nitrogen-centred radicals from lysine residues and their role in protein fragmentation, Biochem. J. 332 (1998) 617–625.
[33] C.L. Hawkins, M.J. Davies, Hypochlorite-induced oxidation of proteins in plasma: formation of chloramines and nitrogen-centred radicals and their role in protein fragmentation, Biochem. J. 340 (1999) 539–548.
[34] A.J. Kettle, Neutrophils convert tyrosyl residues in albumin to chlorotyrosine, FEBS Lett. 379 (1996) 103–106.
[35] A.J. Kettle, A.M. Albrett, A.L. Chapman, N. Dickerhof, L.V. Forbes, I. Khalilova, R. Turner, Measuring chlorine bleach in biology and medicine, Biochim. Biophys. Acta 1840 (2014) 781–793.
[36] S.L. Hazen, J.W. Heinecke, 3-chlorotyrosine, a specific marker of myeloperoxidase-catalysed oxidation, is markedly elevated in low density lipoprotein isolated from human atherosclerotic intima, J. Clin. Investig. 99 (1997) 2075–2081.
[37] B. Shao, C. Bergt, X. Fu, P. Green, J.C. Voss, M.N. Oda, J.F. Oram, J.W. Heinecke, Tyrosine 192 in apolipoprotein a-i is the major site of nitration and chlorination by myeloperoxidase, but only chlorination markedly impairs abca1-dependent cholesterol transport, J. Biol. Chem. 280 (2005) 5983–5993.
[38] B. Shao, S. Pennathur, J.W. Heinecke, Myeloperoxidase targets apolipoprotein a-i, the major high density lipoprotein protein, for site-specific oxidation in human atherosclerotic lesions, J. Biol. Chem. 287 (2012) 6375–6386.
[39] L. Zheng, B. Nukuna, M.L. Brennan, M. Sun, M. Goormastic, M. Settle, D. Schmitt, X. Fu, L. Thomson, P.L. Fox, H. Ischiropoulos, J.D. Smith, M. Kinter, S.L. Hazen, Apolipoprotein a-i is a selective target for myeloperoxidase-catalyzed oxidation and functional impairment in subjects with cardiovascular disease, J. Clin. Investig. 114 (2004) 529–541.
[40] A. Undurti, Y. Huang, J.A. Lupica, J.D. Smith, J.A. DiDonato, S.L. Hazen, Modification of high density lipoprotein by myeloperoxidase generates a pro-inflammatory particle, J. Biol. Chem. 284 (2009) 30825–30835.
[41] T. Nybo, M.J. Davies, A. Rogowska-Wrzesinska, Analysis of protein chlorination by mass spectrometry, Redox Biol. (2018) (submitted for publication).
[42] J.M. Dypbukt, C. Bishop, W.M. Brooks, B. Thong, H. Eriksson, A.J. Kettle, A sensitive and selective assay for chloramine production by myeloperoxidase, Free Radic. Biol. Med. 39 (2005) 1468–1477.
[43] A.J. Kettle, C.C. Winterbourn, Assays for the chlorination activity of myeloperoxidase, Methods Enzymol. 233 (1994) 502–512.
[44] T. Masuda, M. Tomita, Y. Ishihama, Phase transfer surfactant-aided trypsin digestion for membrane proteome analysis, J. Proteome Res. 7 (2008) 731–740.
[45] R.E. Ferguson, H.P. Carroll, A. Harris, E.R. Maher, P.J. Selby, R.E. Banks, Housekeeping proteins: a preliminary study illustrating some limitations as useful references in protein expression studies, Proteomics 5 (2005) 566–571.
[46] K. Tveen-Jensen, A. Reis, L. Mouls, A.R. Pitt, C.M. Spickett, Reporter ion-based mass spectrometry approaches for the detection of non-enzymatic protein modifications in biological samples, J. Proteom. 92 (2013) 71–79.
[47] J. Talib, D.I. Pattison, J.A. Harmer, D.S. Celermajer, M.J. Davies, High plasma thiocyanate levels modulate protein damage induced by myeloperoxidase and perturb measurement of 3-chlorotyrosine, Free Radic. Biol. Med. 53 (2012) 20–29.
[48] H.J. Chen, Y.F. Yang, P.Y. Lai, P.F. Chen, Analysis of chlorination, nitration, and nitrosylation of tyrosine and oxidation of methionine and cysteine in hemoglobin from type 2 diabetes mellitus patients by nanoflow liquid chromatography tandem mass spectrometry, Anal. Chem. 88 (2016) 9276–9284.
[49] E.C. Kennett, M.D. Rees, E. Malle, A. Hammer, J.M. Whitelock, M.J. Davies, Peroxynitrite modifies the structure and function of the extracellular matrix proteoglycan perlecan by reaction with both the protein core and the heparan sulfate chains, Free Radic. Biol. Med 49 (2010) 282–293.
[50] M.D. Rees, J.M. Whitelock, E. Malle, C.Y. Chuang, R.V. Iozzo, A. Nilasaroya, M.J. Davies, Myeloperoxidase-derived oxidants selectively disrupt the protein core of the heparan sulfate proteoglycan perlecan, Matrix Biol. 29 (2010) 63–73.
[51] G. Degendorfer, C.Y. Chuang, A. Hammer, E. Malle, M.J. Davies, Peroxynitrous acid induces structural and functional modifications to basement membranes and its key component, laminin, Free Radic. Biol. Med. 89 (2015) 721–733.
[52] G. Degendorfer, C.Y. Chuang, M. Mariotti, A. Hammer, G. Hoefler, P. Hagglund, E. Malle, S.G. Wise, M.J. Davies, Exposure of tropoelastin to peroxynitrous acid gives high yields of nitrated tyrosine residues, di-tyrosine cross-links and altered protein structure and function, Free Radic. Biol. Med. 115 (2017) 219–231.
[53] G. Degendorfer, C.Y. Chuang, H. Kawasaki, A. Hammer, E. Malle, F. Yamakura, M.J. Davies, Peroxynitrite-mediated oxidation of plasma fibronectin, Free Radic. Biol. Med. 97 (2016) 602–615.
[54] C. Leeuwenburgh, M.M. Hardy, S.L. Hazen, P. Wagner, S. Oh-ishi, U.P. Steinbrecher, J.W. Heinecke, Reactive nitrogen intermediates promote low density lipoprotein oxidation in human atherosclerotic intima, J. Biol. Chem. 272 (1997) 1433–1436.
[55] G. Ferrer-Sueta, N. Campolo, M. Trujillo, S. Bartesaghi, S. Carballal, N. Romero, B. Alvarez, R. Radi, Biochemistry of peroxynitrite and protein tyrosine nitration, Chem. Rev. 118 (2018) 1338–1408.
[56] M.D. Rees, L. Dang, T. Thai, D.M. Owen, E. Malle, S.R. Thomas, Targeted subendothelial matrix oxidation by myeloperoxidase triggers myosin ii-dependent deadhesion and alters signaling in endothelial cells, Free Radic. Biol. Med. 53 (2012) 2344–2356.
[57] S. Vanichkitrungruang, C.Y. Chuang, M.J. Davies, Oxidation of human plasma

fibronectin by hypochlorous (HOCL) and hypothiocyanous (HOSCN) acids perturbs endothelial cell function, Free Radic. Biol. Med. (2018) (submitted for publication).
[58] M.L. Brennan, M.S. Penn, F. Van Lente, V. Nambi, M.H. Shishehbor, R.J. Aviles, M. Goormastic, M.L. Pepoy, E.S. McErlean, E.J. Topol, S.E. Nissen, S.L. Hazen, Prognostic value of myeloperoxidase in patients with chest pain, N. Engl. J. Med. 349 (2003) 1595–1604.
[59] W.H.W. Tang, M.L. Brennan, K. Philip, W. Tong, S. Mann, F. Van Lente, S.L. Hazen, Plasma myeloperoxidase levels in patients with chronic heart failure, Am. J. Cardiol. 98 (2006) 796–799.
[60] R. Zhang, M.L. Brennan, X. Fu, R.J. Aviles, G.L. Pearce, M.S. Penn, E.J. Topol, D.L. Sprecher, S.L. Hazen, Association between myeloperoxidase levels and risk of coronary artery disease, JAMA 286 (2001) 2136–2142.
[61] S.J. Nicholls, W.H. Wilson Tang, D. Brennan, M.L. Brennan, S. Mann, S.E. Nissen, S.L. Hazen, Risk prediction with serial myeloperoxidase monitoring in patients with acute chest pain, Clin. Chem. 57 (2011) 1762–1770.
[62] S. Baldus, C. Heeschen, T. Meinertz, A.M. Zeiher, J.P. Eiserich, T. Munzel, M.L. Simoons, C.W. Hamm, Myeloperoxidase serum levels predict risk in patients with acute coronary syndromes, Circulation 108 (2003) 1440–1445.
[63] V. Rudolph, B.U. Goldmann, C. Bos, T.K. Rudolph, A. Klinke, K. Friedrichs, D. Lau, K. Wegscheider, M. Haddad, T. Meinertz, S. Baldus, Diagnostic value of mpo plasma levels in patients admitted for suspected myocardial infarction, Int. J. Cardiol. 153 (2010) 267–271.
[64] D.I. Pattison, M.J. Davies, C.L. Hawkins, Reactions and reactivity of myeloperoxidase-derived oxidants: differential biological effects of hypochlorous and hypothiocyanous acids, Free Radic. Res. 46 (2012) 975–995.
[65] L. Kubala, H. Kolarova, J. Vitecek, S. Kremserova, A. Klinke, D. Lau, A.L. Chapman, S. Baldus, J.P. Eiserich, The potentiation of myeloperoxidase activity by the glycosaminoglycan-dependent binding of myeloperoxidase to proteins of the extracellular matrix, Biochim. Biophys. Acta 2013 (1830) 4524–4536.
[66] S. Baldus, J.P. Eiserich, A. Mani, L. Castro, M. Figueroa, P. Chumley, W. Ma, A. Tousson, T.C.R. White, D.C. Bullard, M.-L. Brennan, A.J. Lusis, K.P. Moore, B.A. Freeman, Endothelial transcytosis of myeloperoxidase confers specificity to vascular ecm proteins as targets of tyrosine nitration, J. Clin. Investig. 108 (2001) 1759–1770.
[67] U. Schwarz-Linek, J.M. Werner, A.R. Pickford, S. Gurusiddappa, J.H. Kim, E.S. Pilka, J.A. Briggs, T.S. Gough, M. Hook, I.D. Campbell, J.R. Potts, Pathogenic bacteria attach to human fibronectin through a tandem beta-zipper, Nature 423 (2003) 177–181.
[68] G.A. Homandberg, J. Kramer-Bjerke, D. Grant, G. Christianson, R. Eisenstein, Heparin-binding fragments of fibronectin are potent inhibitors of endothelial cell growth: structure-function correlations, Biochim. Biophys. Acta 874 (1986) 61–71.
[69] E. Makogonenko, G. Tsurupa, K. Ingham, L. Medved, Interaction of fibrin(ogen) with fibronectin: further characterization and localization of the fibronectin-binding site, Biochemistry 41 (2002) 7907–7913.
[70] H. Ni, P.S. Yuen, J.M. Papalia, J.E. Trevithick, T. Sakai, R. Fassler, R.O. Hynes, D.D. Wagner, Plasma fibronectin promotes thrombus growth and stability in injured arterioles, Proc. Natl. Acad. Sci. USA 100 (2003) 2415–2419.
[71] A. Sharma, J.A. Askari, M.J. Humphries, E.Y. Jones, D.I. Stuart, Crystal structure of a heparin- and integrin-binding segment of human fibronectin, EMBO J. 18 (1999) 1468–1479.
[72] R. Pytela, M.D. Pierschbacher, E. Ruoslahti, Identification and isolation of a 140 kd cell surface glycoprotein with properties expected of a fibronectin receptor, Cell 40 (1985) 191–198.
[73] A. Woods, J.R. Couchman, S. Johansson, M. Hook, Adhesion and cytoskeletal organisation of fibroblasts in response to fibronectin fragments, EMBO J. 5 (1986) 665–670.
[74] L. Bloom, K.C. Ingham, R.O. Hynes, Fibronectin regulates assembly of actin filaments and focal contacts in cultured cells via the heparin-binding site in repeat iii13, Mol. Biol. Cell 10 (1999) 1521–1536.
[75] A. Woods, J.R. Couchman, Syndecan-4 and focal adhesion function, Curr. Opin. Cell Biol. 13 (2001) 578–583.
[76] Y. Mahalingam, J.T. Gallagher, J.R. Couchman, Cellular adhesion responses to the heparin-binding (hepii) domain of fibronectin require heparan sulfate with specific properties, J. Biol. Chem. 282 (2007) 3221–3230.
[77] S.T. Lim, R.L. Longley, J.R. Couchman, A. Woods, Direct binding of syndecan-4 cytoplasmic domain to the catalytic domain of protein kinase c alpha (pkc alpha) increases focal adhesion localization of pkc alpha, J. Biol. Chem. 278 (2003) 13795–13802.
[78] J.R. Couchman, Syndecans: proteoglycan regulators of cell-surface microdomains? Nat. Rev. Mol. Cell Biol. 4 (2003) 926–937.
[79] M.D. Bass, M.J. Humphries, Cytoplasmic interactions of syndecan-4 orchestrate adhesion receptor and growth factor receptor signalling, Biochem. J. 368 (2002) 1–15.
[80] E.S. Wijelath, S. Rahman, M. Namekata, J. Murray, T. Nishimura, Z. Mostafavi-Pour, Y. Patel, Y. Suda, M.J. Humphries, M. Sobel, Heparin-ii domain of fibronectin is a vascular endothelial growth factor-binding domain: enhancement of vegf biological activity by a singular growth factor/matrix protein synergism, Circ. Res. 99 (2006) 853–860.
[81] J.H. Kim, S.O. Park, H.J. Jang, J.H. Jang, Importance of the heparin-binding domain of fibronectin for enhancing cell adhesion activity of the recombinant fibronectin, Biotechnol. Lett. 28 (2006) 1409–1413.
[82] K. Briknarova, M.E. Akerman, D.W. Hoyt, E. Ruoslahti, K.R. Ely, Anastellin, an fn3 fragment with fibronectin polymerization activity, resembles amyloid fibril precursors, J. Mol. Biol. 332 (2003) 205–215.
[83] R. You, R.M. Klein, M. Zheng, P.J. McKeown-Longo, Regulation of p38 map kinase by anastellin is independent of anastellin's effect on matrix fibronectin, Matrix Biol. 28 (2009) 101–109.
[84] R. Kinsey, M.R. Williamson, S. Chaudhry, K.T. Mellody, A. McGovern, S. Takahashi, C.A. Shuttleworth, C.M. Kielty, Fibrillin-1 microfibril deposition is dependent on fibronectin assembly, J. Cell Sci. 121 (2008) 2696–2704.
[85] J.A. McDonald, D.G. Kelley, T.J. Broekelmann, Role of fibronectin in collagen deposition: fab' to the gelatin-binding domain of fibronectin inhibits both fibronectin and collagen organization in fibroblast extracellular matrix, J. Cell Biol. 92 (1982) 485–492.